An Analysis of Arctic Sea Ice Fluctuations, 1953–77

JOHN E. WALSH AND CLAUDIA M. JOHNSON

Laboratory for Atmospheric Research, University of Illinois, Urbana 61801

(Manuscript received 8 August 1978, in final form 26 October 1978)

ABSTRACT

Arctic sea ice data from the 1953–77 period are digitized onto a set of 300 monthly grids covering the polar cap. Each grid contains 1648 ice concentration points at a spacing of 1° latitude (60 n mi). The synthesis of the regional ice data sets is described.

The digitized data are used to evaluate quantitatively the normal seasonal cycle of ice extent, the 25 year extremes for winter and summer, and the longitudinal dependence of the variance and trend of ice extent. Interannual variations of ice extent exceeding 5° latitude are found at most longitudes. The time series of total Arctic ice extent shows a statistically significant positive trend and correlates negatively with recent high-latitude temperature fluctuations.

Empirical orthogonal functions of longitude are used to identify the major spatial and temporal scales of ice fluctuations within the 25-year period. The dominant spatial mode is an asymmetric mode in which the North Atlantic anomaly is opposite in sign to the anomaly over the remainder of the polar cap. A tendency for ice anomalies to persist for several months is apparent in the lagged autocorrelations of the amplitudes of the dominant ice eigenvectors. The month-to-month persistence of the ice anomalies is considerably greater than the persistence of the high-latitude meteorological anomaly fields of sea level pressure, surface temperature and 700 mb height.

1. Introduction

Substantial year-to-year variations in the extent of sea ice have been observed in nearly every geographical sector of the Arctic. Winchester and Bates (1958), for example, describe cases in which the September position of the ice edge north of Alaska differed by several hundred kilometers in successive years. Fluctuations of a similar magnitude have been noted north of Iceland (Björnsson, 1969), in Baffin Bay and Davis Strait (Dunbar, 1972), in the North Atlantic Ocean and the Barents and Norwegian Seas (Haupt and Kant, 1976), and in the Soviet Arctic (Volkov and Sleptsov-Shevlevich, 1971). These interannual variations in ice extent have several consequences. First, they can seriously effect navigability in the vicinity of the ice edge. Because large portions of the North American and Eurasian coastal waters are ice-covered during much of the year, the feasibility of shipping operations in a particular year is often quite unpredictable. Dehn (1972), for example, summarizes the hazards posed by ice in the Alaskan shipping corridor. Perhaps more importantly, sea ice plays a crucial role in the energy budget of the Arctic by reflecting large fractions of the incoming solar radiation and by effectively insulating the atmosphere from the underlying ocean. It has been speculated (e.g., Fletcher, 1968; Budyko, 1972) that large-scale variations in the sea ice cover may be climatically significant. The effect of ice extent on interannual atmospheric variations has been the subject of recent studies by Ackley and Keliher (1976) and Herman and Johnson (1978). Ackley and Keliher examined two years of Antarctic data and noted some possible effects of the sea ice distribution on the atmospheric circulation near the Antarctic periphery. In the Herman and Johnson study, the GISS[1] general circulation model was found to exhibit a statistically significant response to prescribed changes in the January extent of Arctic sea ice.

The verification of modeled ice/atmosphere interactions and the development of improved ice forecasts for shipping concerns requires a relatively uniform data base depicting ice variations over as long a time period as possible. However, as implied by the variety of studies mentioned in the previous paragraph, the existing data on sea ice extent have been collected and analyzed primarily on a regional basis. Only since the advent of satellite observations in the late 1960's has a uniform set of ice data been available for the entire polar region. Data from the "satellite era" have formed the basis for recent studies by Sanderson (1975) and Kukla (1978). In the former, ice charts compiled by the British Meteorological Office were used to examine variations in ice extent during the 1966–74 period. The areal extent of ice in five longitudinal sectors was determined

[1] Goddard Institute for space studies.

0022-3670/79/030580-12$07.00

by planimetry for three winter and two summer months of each year. Less ice was found in the 1972–74 period than in the earlier part of the study period. Kukla, whose data included snow as well as ice extent for the 1968–76 period, shows a substantial increase in snow/ice coverage between 1971 and 1973 followed by a gradual decrease through 1975. The apparent discrepancy in the results of these two studies is most likely attributable to the fact that Kukla included snow data, whereas Sanderson did not. Other factors may be Sanderson's use of the 7/10 concentration line as the ice/no-ice boundary and the omission of areas such as the southern Bering Sea from the British ice charts.

The present work is an analysis of sea ice fluctuations computed from a data set that has been synthesized from a variety of regional data sources as well as the more recent satellite-derived hemispheric analyses. The 300-month record length of the resulting data set is longer than those of the compilations used by Sanderson and Kukla, while the spatial resolution is finer. Section 2 describes the data set and its construction. Section 3 is a quantitative evaluation of the spatial and temporal scales of the fluctuations of ice extent computed from the digitized data set. The variance of the area of ice-covered ocean is evaluated as a function of longitude, and the 25-year extremes are depicted in the form of composite maxima and minima. The longitudinal dependence of the trend in ice extent over the 25-year period is also shown. Empirical orthogonal functions are then constructed in order to isolate the dominant spatial modes of variability of ice extent. Lagged autocorrelations of the coefficients of the dominant eigenvectors are used to illustrate the time scales of the ice anomalies. These time scales are then compared with those of the high-latitude meteorological anomaly fields.

2. The sea-ice data set

Monthly ice concentration grids were compiled from existing data on the observed distribution of sea ice. The data sources are listed in Table 1. The concentration grid (see Fig. 1) consists of 1648 ice data points separated by 60 n mi (1° latitude); the positive x and y axes are 20°W and 70°E. The grid covers those portions of the high-latitude oceans where ice was observed during any month of the study period. The 1° spacing was chosen because it permits the resolution of year-to-year fluctuations. Finer resolution would have added substantially to the labor involved in the digitization and would not have been justified by the quality of much of the earlier data.

The grid-point values are the fractions (tenths) of each grid area covered by ice. A separate array containing the ocean area corresponding to each grid point is stored in digital form for use in computations of the ice-covered ocean area in various latitude or longitude bands. The ocean areas are rounded to the nearest tenth of a squared latitude degree.

TABLE 1. Ice data sources, listed in order of the most recent.

U.S. Navy Fleet Weather Facility, 1976–77: Arctic Sea Ice Analyses, Eastern and Western (weekly charts), Suitland, MD.
——, 1976a: Eastern Arctic Sea Ice Analyses, 1972–75. ADA 033344, Suitland, MD.
——, 1976b: Western Arctic Sea Ice Analyses, 1972–75. ADA 033345, Suitland, MD.
British Meteorological Office, 1959–77: Monthly Ice Charts, HMSO, London (1959 charts in *Mariners Weather Log*, vols. 3–4).
U.S. Naval Oceanographic Office, 1953–71: *Report(s) of the Arctic Ice Observing and Forecasting Program*. Tech. Reps. TR-49 through TR-52, TR-66, TR-69; Spec. Pubs. SP-70 through SP-81, Washington, DC.
Canadian Meteorological Service, 1966–71: *Ice Summary and Analysis*, 1964–69 (Yearbooks), Toronto, Ontario.
Arbok Norsk Polarinstitut, Oslo, 1963–71: Sea ice and drift speed observations (Annual reports). Also, T. Lunde, 1965: Ice conditions at Svalbard, 1946–1963, *Arbok Norsk Polarinstitut* (1963).
Danish Meteorological Institute, 1957–1968: *The Ice Conditions in the Greenland Waters* (Yearbooks), Charlottenlund, Copenhagen.
U.S. Navy Hydrographic Office, 1958: *Oceanographic Atlas of the Polar Seas. Part II. Arctic*. H. O. Publ. No. 705, Washington, DC.
Danish Meteorological Institute, 1953–56: The state of the ice in the Arctic Seas. Appendices to *Nautical-Meteorological Annuals* (Yearbooks), Charlottenlund, Copenhagen.
Jökull, 1953–67: Reports of sea ice off the Icelandic coasts (Annual reports). Icelandic Glaciological Society, Reykjavik.

The grids were constructed for the end of each month of the 1953–77 period. 1953 was chosen as the starting date because it represents the beginning of an essentially continuous data record for the North American Arctic. For each month, data from the various sources were transcribed to a master grid which was then digitized. An example of a concentration grid in digital form is shown in Fig. 2. The 300 monthly grids and the ocean area grid are stored on tape at the National Center for Atmospheric Research.

The obvious advantage of a data synthesis such as this one is that the record length is considerably greater than it would be if only data from the satellite era were included. The major disadvantage is that the data are less homogeneous in space and time, especially during the early portion of the study period. The factors contributing to the risk of some nonuniformity in the synthesized data set include the following:

1) IMPRECISE CONCENTRATION CLASSIFICATIONS

Since ice conditions can vary considerably over relatively small areas, several ice-observing agencies have tended to group the ice concentrations

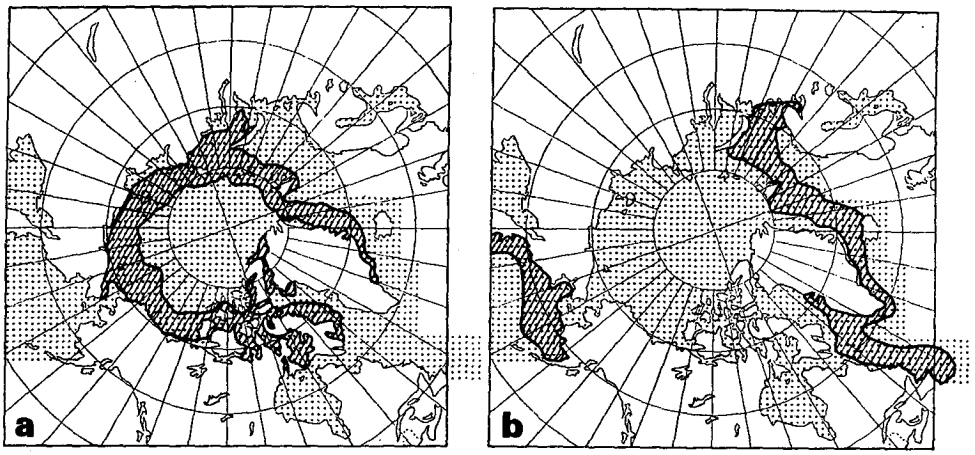

FIG. 1. Composite maximum and minimum ice extent at the end of August (a) and February (b). Heavy lines are extreme positions of 0.5 ice concentration lines based on the 25 August grids and the 25 February grids (1953–77). Dots represent grid points used in digitization of monthly ice concentration data.

into categories. The British Meteorological Office, for example, uses categories such as "very open" (1/10–3/10) and "open" (4/10–6/10). The charts of the Canadian Meteorological Service and the U.S. Naval Oceanographic Office are based on similar classifications, although both these sources superimpose specific concentration values on their charts when the data permit precision. In areas where only concentration categories were indicated on the source charts, the digitized values used in this work are the means of the concentrations in each category, rounded upward if necessary. For example, the very open and open categories of the British charts are stored as 2/10 and 5/10, respectively, while the 5/10–8/10 category of the U.S. Naval Oceanographic Office is stored as 7/10.

2) INCONSISTENCIES IN OVERLAPPING DATA

When data from more than one source were available for the same region and the same time, occasional discrepancies in the charted concentration fields were noted. The digitized values in such cases are means of the different charted values unless one data source was at variance with two or more consistent sources. In the latter case, the inconsistent data source was ignored.

3) MISSING DATA

For some months in the early part of the study period, no data were available for certain areas. In particular, there were no data for the Siberian sector during several years in the 1950's. While winter concentrations can be assumed to be 10/10 in this region, the summer values are unknown. In such cases the grid point values are either (i) concentrations linearly interpolated from the preceding and following months if data for both the preceding and following months were available; or (ii) mean concentrations for the particular month if data for either the preceding or following months were not available. The mean concentrations in these cases were computed using the subset of the 25 monthly grids for which data were available at the point in question. This strategy will tend to reduce the variance and trends computed for the grid point or region.

In cases where the data values are estimates because of these three factors, the stored digital values are "tagged" as estimates. The option to ignore such values is therefore available to users of the data.

3. Results of the data analysis

The data set described in Section 2 was used to evaluate the spatial and temporal scales of fluctuations in ice extent over the past 25 years (1953–77). Ice extent is defined in this study as the area covered by sea ice, regardless of ice thickness or stage of development. The ice extent in a region is therefore the sum (over all grid points in the region) of the products of the grid-point concentrations and their corresponding ocean areas. Ice extent defined in this manner is not equivalent to the area enclosed by a single boundary or ice concentration contour. Estimated concentration values were included in the computations.

Since this work is a study of the variability of the main Arctic ice pack, data were included for the Arctic Ocean and the adjacent bodies of water: the Barents, White, Kara, Laptev, East Siberian, Chukchi, Bering and Beaufort Seas, Hudson Bay and the waters of the Canadian Archipelago, Davis Strait, Baffin Bay, Denmark Strait and the East Greenland Sea. Data for the Sea of Okhotsk and the

Baltic Sea were not included because these two water bodies (unlike Hudson Bay, for example) are separated from the Arctic Seas by continuous landmasses and are not bounded by any of the water bodies listed above. The only area not included in the study although it does border on an included area is the Gulf of St. Lawrence. Since data for the Gulf of St. Lawrence were available for less than half of the 25-year period, it was felt that the inclusion of this area would add little to the data analysis.

Fig. 3 is a plot of the normal seasonal cycle of the area covered by sea ice. The data points represent 25-year averages of the end-of-the-month values of ice extent in all areas except those noted above. Fig. 3 shows that the ratio of the maximum ice area (late February, early March) to the minimum ice area (late August, early September) is approximately 2.0. This value, which admittedly suffers from the bias introduced by the selective inclusion of the peripheral seas listed in the preceding paragraph, is about 10% larger than the corresponding ratio obtained from Untersteiner's (1975, p. 206) values of ice areas for the Arctic Ocean. The maximum/minimum ratio obtained here would have been even larger had the Baltic Sea, the Sea of Okhotsk and the Gulf of St. Lawrence been included, since these three water bodies are ice-free in the late summer. Fig. 3 also shows that the autumn increase

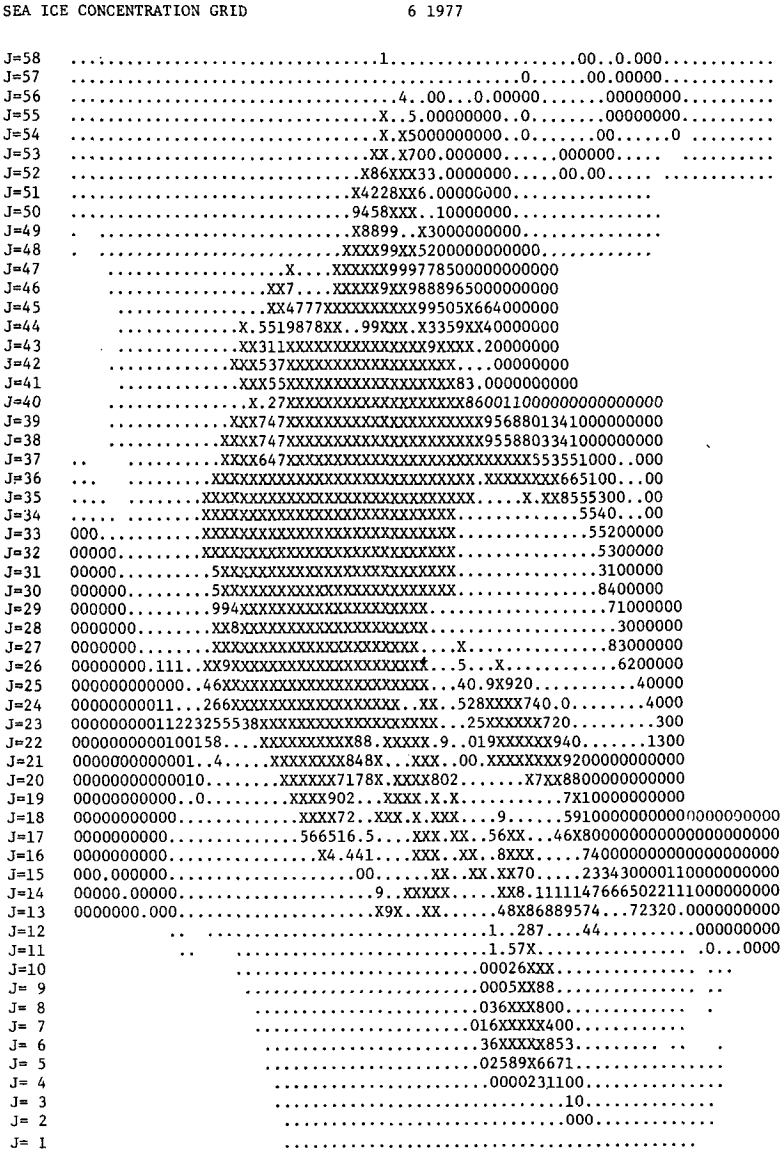

FIG. 2. Sample ice grid (June 1977) in digital form. Integers 0, 1, . . . , 9 give ice coverage in tenths; X's represent 10/10 ice coverage; dots are grid points located over land.

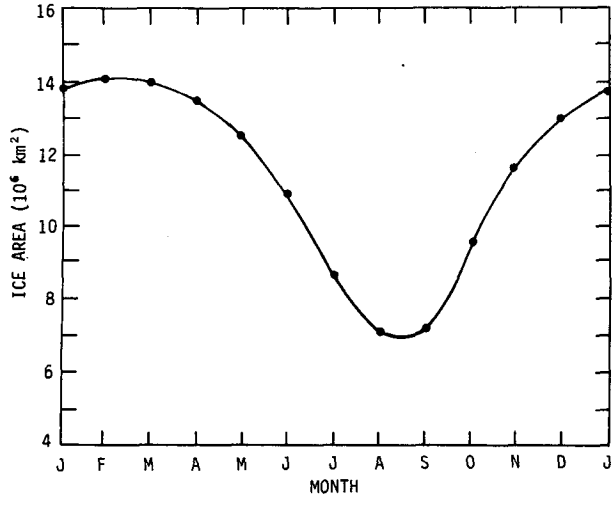

FIG. 3. The normal seasonal cycle of Arctic sea ice extent. Heavy dots are 25-year averages of area covered by ice at end of month.

of ice area is slightly more rapid than the decrease during spring and summer.

The interannual variability of ice extent at the approximate times of the minimum and maximum ice extent can be seen in Fig. 1, which shows the composites of the ice extremes determined from the set of 25 August grids and the set of 25 February grids. The composite maxima and minima are defined as the positions of the 0.5 concentration lines in the lightest and heaviest ice years at each longitude. It is apparent that the 25-year variability of both winter and summer ice extent is approximately 5° of latitude at all longitudes where the ice advance is not limited by the continental landmasses. It might be noted that the North Atlantic portion of the shaded area of Fig. 1b is comparable to the area between the *mean* position of the early spring boundary of North Atlantic "ice extent" in the early 1800's and the corresponding *mean* position in the early 1900's (Lamb, 1972, p. 338). Since Lamb does not define "ice extent" in terms of ice concentrations, further comparisons with the results of the present study cannot be made.

The tendency for the continents to reduce the interannual variance of ice extent can be seen in Fig. 4, which is a plot of the standard deviation of the departure from the monthly mean ice-covered area of each 20° longitudinal sector. All 300 monthly grids were used in this computation. The standard deviations of ice area are largest in the Bering Sea, in the Baffin Bay-Davis Strait area, and in the North Atlantic Ocean northeast of Iceland. Such a longitudinal distribution of variance might have been anticipated from Fig. 1 because the 12-month averages of the anomaly magnitudes are reduced by the zero winter variance in those areas where the ice advance is blocked by the continental landmasses (e.g., Siberia, North America).

Fig. 5 shows the time series of the departures from the monthly means of the area covered by Arctic sea ice. While the unsmoothed plot (Fig. 5a) shows that there is considerable fluctuation about the mean within most years, some general features of the smoothed plot (Fig. 5b) are worth noting. The general minimum of iciness in the early 1960's was followed by a fairly sharp increase during the mid-1960's. Ice extent then remained generally above normal for 5–8 years. The decrease in ice extent during the early 1970's is in general agreement with the previously mentioned results of Sanderson (1975). Fig. 5b shows that the first part (1967–71)

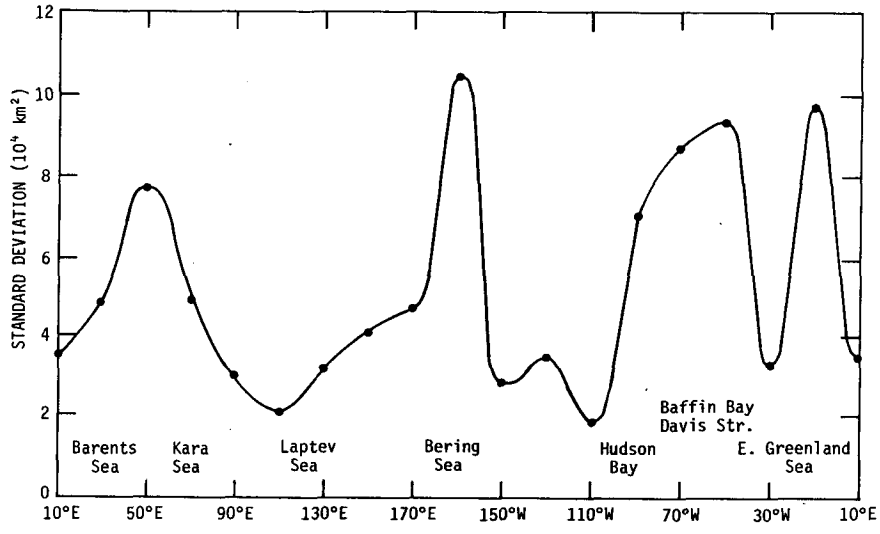

FIG. 4. Longitudinal dependence of the standard deviation (10^4 km^2) of the departure from the monthly mean areal extent of sea ice.

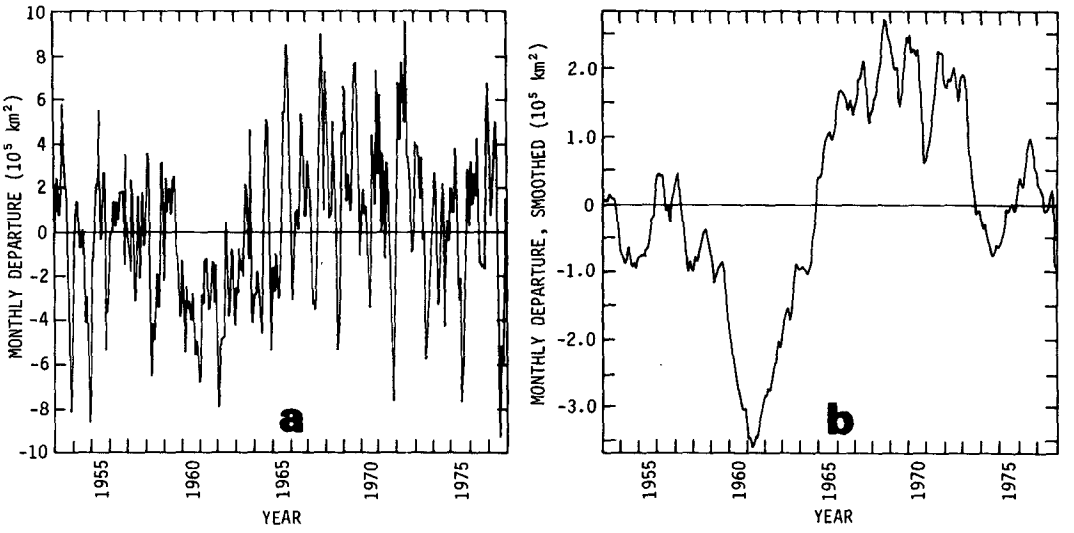

FIG. 5. 300-month time series of the departures from the monthly means of the area covered by Arctic sea ice, showing unsmoothed values (a) and 24-month running means (b).

of Sanderson's study period was the iciest of the past 25 years, and that the subsequent decrease in ice extent was merely a return to the 25-year mean. The sharp increase in (combined) snow and ice extent during 1971–73, reported by Kukla (1978), is not apparent in Fig. 5b. However, in view of the large spatial variations of snowcover over land, the comparison with Kukla's results is most likely inappropriate.

The recent trend of Arctic ice extent, computed as the slope of the linear regression line fitted by least squares to the 300 monthly values of Fig. 5a, is 3.14×10^3 km^2 year^{-1}. An increase in ice extent over the 25-year period is therefore indicated. The significance of this trend can be estimated from the ratio S of the computed slope to the standard deviation of the slope to be expected when samples of the same size are drawn from an infinite series of randomly distributed values having the same variance as the (unsmoothed) series; S is therefore a measure of the extent to which the trend computed from a finite series is attributable to one or two large fluctuations near the extremes of the series (van Loon and Williams, 1977). The S-value of the slope of Fig. 5a is 3.30, implying that the slope is more than three times the standard deviation of the slope to be expected from a random series.

Fig. 6 shows the time series (24-month running mean) of the area-averaged surface temperature for the polar cap north of 60°N. The plot was constructed by adding data for the years 1976 and 1977 to the temperature data set described by Walsh (1977). The slope of the linear regression line fitted to the temperature series is negative, implying a net temperature decrease over the past 25 years; the unsmoothed temperature series was used to compute a significance value of $S \approx 2.5$ for the 1953–77 temperature trend. A comparison of Figs. 5b and 6 reveals some corresponding features. Above-normal temperatures during 1959–62 were followed by a rather pronounced cooling to a 1965 minimum. The increase in ice extent during the cool period is apparent in Fig. 5b. A return to the 25-year mean by the mid-1970's is seen in both the temperature and the ice plots. Lagged correlations of the two series will be discussed after the temporal and spatial modes of the two variables are compared.

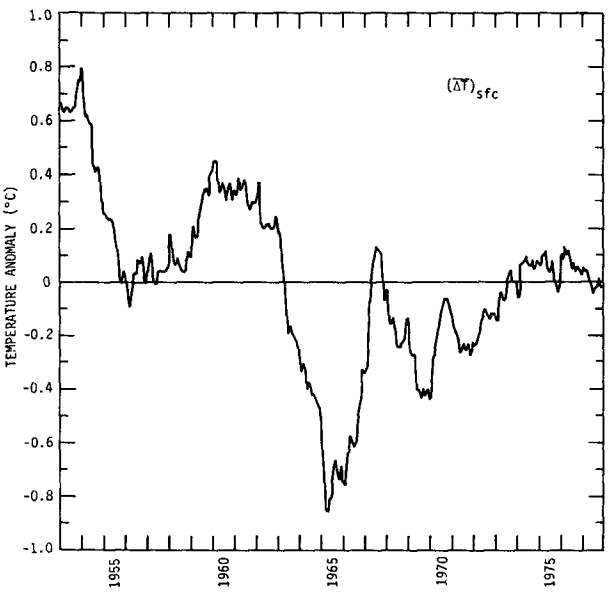

FIG. 6. Time series (24-month running mean) of the departure (°C) from 25-year normal of the area-weighted temperature of the polar cap north of 60°N.

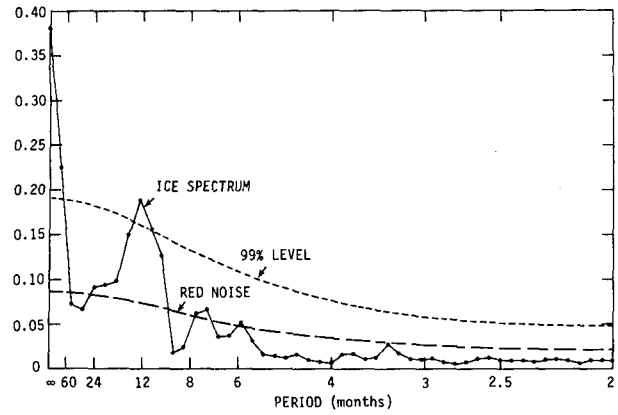

FIG. 7. Normalized frequency spectrum of the departure from the monthly mean of the area covered by Arctic sea ice. Also shown is the red noise continuum (dashed line) and the associated 99% confidence limit (dotted line).

The frequency spectrum of the time series of Fig. 5a is plotted in Fig. 7. Also shown is the corresponding red noise continuum computed from the serial correlation coefficient (=0.655) at lag 1, together with the associated 99% confidence limit (Mitchell *et al.*, 1966, p. 36). The spectral peak at 12 months is significant at the 99% level. A rather straightforward interpretation of this peak is that the summer variance exceeds the winter variance due to the lack of interannual winter variability along the northern coastlines of Northern America and Asia. The summer data therefore contain more scatter than the winter data. It should be added that the 25-year period used in this study is evidently too short to provide statistical verification of the apparent 2–7 year cycles noted in the Soviet data by Volkov and Sleptsov-Shevlevich (1971) and the 5-year cycle noted in Alaskan data by Barnett (1979).

Fig. 8 shows the longitudinal dependence of the trend of ice extent over the 300 months. Considerable longitudinal variation is apparent. The net positive trend of Fig. 5 is evidently due to increased iciness in the regions of Baffin Bay, Davis Strait, the East Greenland Sea and, to a lesser extent, the coastal waters of Alaska. The data indicate that iciness has decreased in the Barents Sea.

Since the emphasis of this work is on the spatial and temporal scales of the departures from normal ice extent, the departure fields are represented in terms of empirical orthogonal functions. These functions have the advantage that they are the most efficient possible data representations in the sense that the dominant orthogonal functions account for more of the variance of a set of data fields than any other combination of the same number of parameters or functions. Davis (1976, Appendix B) outlines the formulation of empirical orthogonal functions, which are also referred to as eigenvectors or principal components. A relatively nonmathematical discussion of the construction and interpretation of eigenvectors is given by Stidd (1967). Eigenvectors have been used to represent meteorological fields by a number of investigators (e.g., Kutzbach, 1967) and to describe sea-surface temperature anomalies by Davis (1976), Weare *et al.* (1976) and Trenberth (1975).

Because the majority of the grid points in Fig. 1 are either totally ice-free or ice-covered throughout the year, the representation of the Arctic ice fluctuations in terms of eigenvectors is formulated somewhat differently from the more common two-dimensional representations of meteorological and sea surface temperature fields. The vector construction used here is based on a partitioning of every grid into 36 variables, each of which is the area covered by ice in a 10° longitudinal sector. The spatial fluctuations are therefore represented in terms of 36 eigenvectors that are orthogonal functions of longitude only. Symbolically, the data matrix **F** is

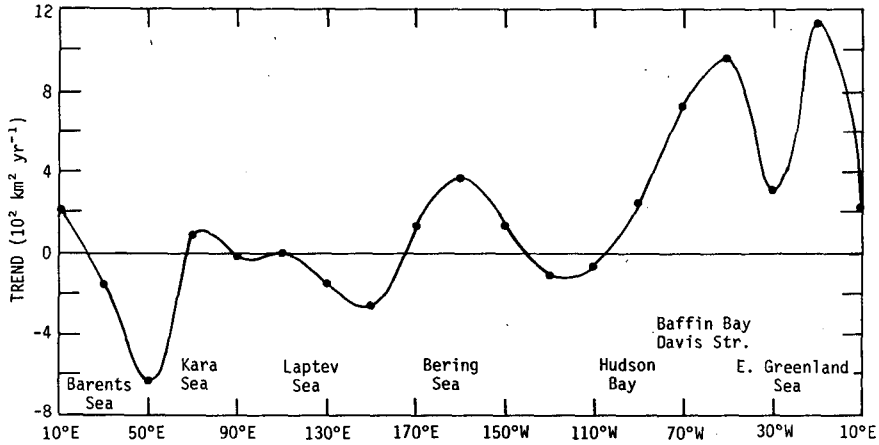

FIG. 8. Longitudinal dependence of the trend (10^2 km^2 year^{-1}) of ice extent. Trends are slopes of least-squares lines fitted to the time series of departures from the monthly means in each 20° longitudinal sector.

$$\mathbf{F} = \begin{pmatrix} f_{11} & f_{21} & f_{I1} \\ f_{12} & f_{22} & f_{I2} \\ \vdots & \vdots \cdots \vdots & \\ f_{1J} & f_{2J} & f_{IJ} \end{pmatrix}, \quad (1)$$

where f_{ij} is the ice-covered area in the jth 10° longitudinal sector during the ith month of the 300-month series. The maximum values of the subscript indices are $I = 300$ and $J = 36$. The normalized data matrix $\hat{\mathbf{F}}$ can then be constructed from $\mathbf{F}$ according to

$$\hat{f}_{ij} = \frac{f_{ij} - \mu_{mj}}{\sigma_j}, \quad (2)$$

where $\hat{f}_{ij}$ is the normalized value of f_{ij}, μ_{mj} the 25-year mean value of the ice area in sector j for the particular month (m) of the year, and σ_j the standard deviation of the ice area in sector j (computed from the entire set of 300 grids). The 36 × 36 correlation matrix obtained from $\hat{\mathbf{F}}$ is then used to compute the eigenvectors and corresponding eigenvalues (see Davis, 1976). The subtraction of the monthly mean in (2) removes the seasonal cycle from the data, thereby assuring that the computed eigenvectors represent patterns of the monthly anomalies or departures from the monthly means. When μ_{mj} is not subtracted from each f_{ij}, the first computed eigenvector represents simply the normal seasonal cycle (anomalies of the same sign at all longitudes) and accounts for over 80% of the variance. The division by σ_j in (2) incorporates the longitudinal distribution of the variance into the formulation. Consequently, the fluctuations in the longitudes having smaller values of σ_j are weighted more heavily in the eigenvector construction than they would be if the data were not normalized. Heavier weighting is therefore assigned to the spring, summer and autumn fluctuations in longitudes where the winter variance is zero, since small winter variances tend to reduce the (12-month average) values of σ_j. (Eigenvectors were constructed from both normalized and non-normalized ice data. While the features of the non-normalized vectors were longitudinally narrower, the general character of the two eigenvector sets was very similar). The anomaly patterns will be discussed here in terms of the normalized eigenvectors because the corresponding meteorological eigenvectors (discussed later) were also computed from normalized data.

Fig. 9 shows the first four eigenvectors of normalized ice extent. For consistency with Figs. 4 and 8, the eigenvector components are plotted at 20° intervals of longitude. These four vectors account for ~45% of the total variance. Since the variance fractions described by the first 6, 12 and 18 of the 36 eigenvectors are 0.56, 0.76 and 0.88, respectively, the eigenvector representation allows the data to be compressed considerably.

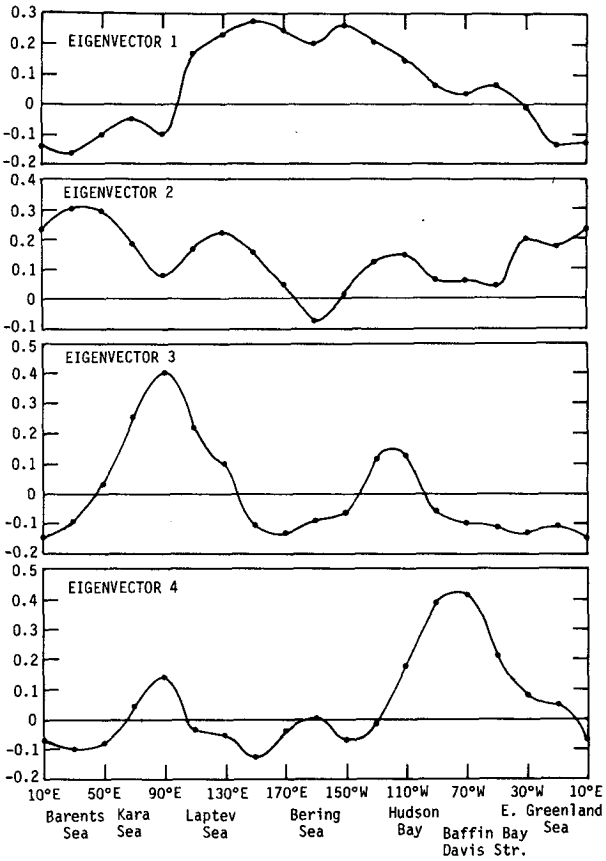

FIG. 9. The first four eigenvectors of normalized ice extent. Horizontal axis is longitude.

The first eigenvector, which might be termed a wavenumber 1 mode, describes fluctuations characterized by an out-of-phase relationship between the North Atlantic/Norwegian Sea/Barents Sea area (east of 40°W) and the remainder of the polar cap. Since this mode describes more variance than any other mode, we may refer qualitatively to the results of van Loon and Rogers (1978, Fig. 9) and Walsh (1977, Fig. 2a), both of which indicate the predominance of an inverse relationship between the surface temperatures of the Eastern North Atlantic/Northern Europe area and the remainder of the high-latitude portion of the northern hemisphere. As shown later in this section, however, the time scales of the surface temperature anomalies are considerably shorter than those of the ice anomalies.

The second eigenvector in Fig. 9 is characterized by anomalies of the same sign at nearly all longitudes. Only a 30° segment of the Alaskan Arctic has anomalies of the opposite sign. The third eigenvector depicts a double-wave pattern in which the anomalies in the Siberian Arctic and in the Beaufort Sea/Western Canada area are in phase. The fourth eigenvector contains large anomalies in the Eastern Canadian waters. A tendency toward a

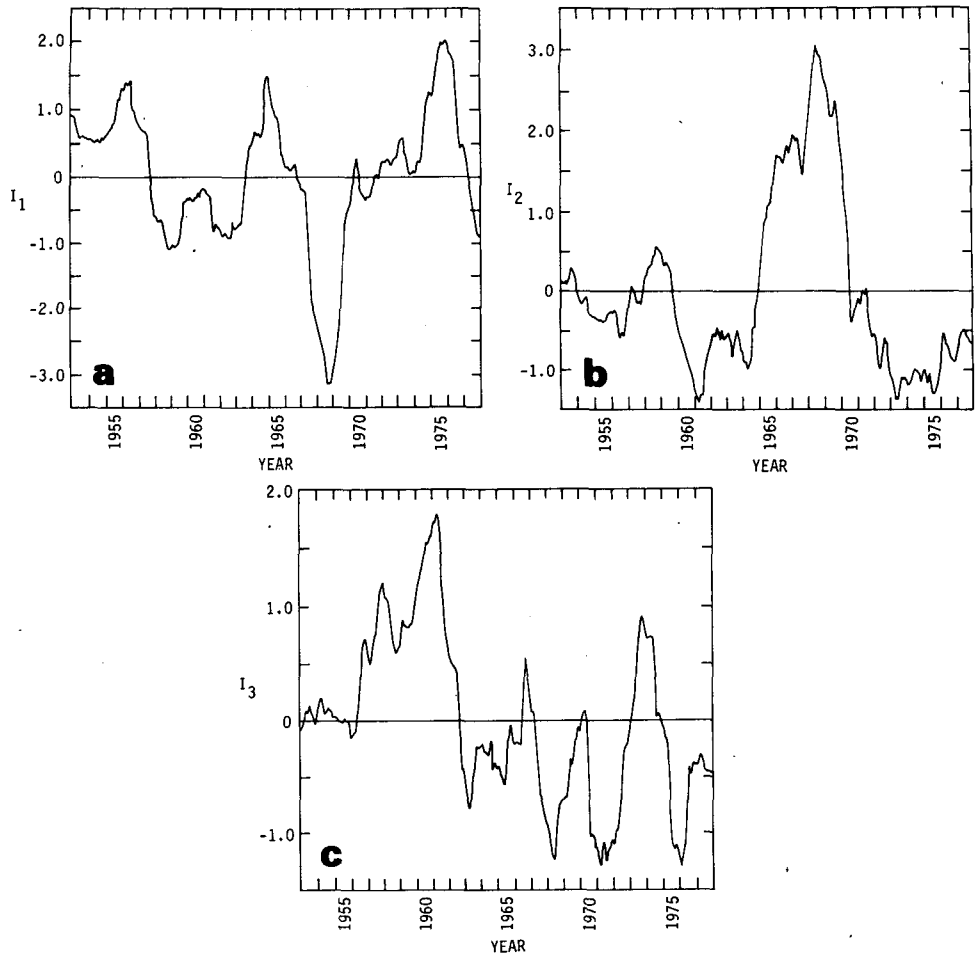

FIG. 10. Time series (24-month running means) of the coefficients of the first three eigenvectors of normalized ice extent: (a) I_1, (b) I_2 and (c) I_3. The abscissa is time and the ordinate is dimensionless in each plot.

finer longitudinal structure is found in the higher eigenvectors.

Fig. 10 shows the 300-month time series (24-month running means) of the coefficients I_1, I_2 and I_3 of the first three eigenvectors. The major feature of the I_1 series is the brief but sharp drop during 1967–68. The linear trend, which is the slope of the least-squares fit to the entire I_1 series, is not statistically significant (S = 0.24). The coefficient I_2 shows an increase in the mid-1960's that resembles the increase in the total ice area (Fig. 5b). This similarity is not surprising since I_2 is characterized by ice anomalies that are of the same sign over nearly the entire Arctic. Because I_2 decreases fairly abruptly in the late 1960's and early 1970's, the 300-month trend (slope) is not statistically significant ($S = 0.72$). However, the slope of the least-squares fit to the I_3 series is -0.004 mo^{-1}, which is 3.29 times the standard deviation of the slope to be expected from the corresponding random series. Superimposed on the gradual decrease of I_3 are frequent substantial departures of both signs from the 300-month mean.

Frequency spectra were also computed for the time series of the first four eigenvector coefficients. Only a spectral peak in I_2 at approximately 12 months, corresponding to the 12-month peak in Fig. 7, was found to be statistically significant at the 95% level. Plots of the spectra will therefore not be shown here.

The persistence of the ice anomalies was evaluated by computing the lagged autocorrelations of the coefficients of the dominant eigenvectors of ice extent. The autocorrelations of the first four coefficients are shown in Fig. 11. The tendency for ice anomalies to persist for several months is apparent. If the curves of Fig. 11 are weighted by the fractions of the four-eigenvector variance described by each individual eigenvector, the weighted mean autocorrelations are 0.636 at one month, 0.390 at two months and 0.233 at three months. The corresponding values for the non-normalized eigenvectors are 0.603, 0.410 and 0.329.

The time series of the coefficients discussed above were used to compute the cross-correlations at lags

0–12 months. The magnitudes of several cross-correlations exceeded 0.2 in portions of the 0–12 month lag range. $\langle I_1 I_2 \rangle$, for example, varied between −0.30 and −0.35 at 2-, 3- and 4-month lags of I_2. The magnitude of all cross correlations were smaller than 0.36, however, and none were statistically significant at the 99% level.

Finally, the time scales of the ice anomalies are compared with those of the high-latitude meteorological anomalies in Fig. 12. The time scales described here are simply the values of the persistence of the departures from the monthly means. The persistence is evaluated as the variance-weighted autocorrelation of the coefficients of the first four (normalized) eigenvectors of sea ice extent, atmospheric sea level pressure, 700 mb height and surface temperature. The three sets of meteorological eigenvectors, described by Walsh (1978), were constructed from 24 years (1952–75) of monthly meteorological data covering the polar cap north of 60°N. The meteorological autocorrelations decay considerably more rapidly than do the sea ice autocorrelations. At one month, for example, the autocorrelations are 0.64 for sea ice and 0.12, 0.28 and 0.18 for the atmospheric fields of sea level pressure, surface temperature and 700 mb height. The implication is that the time scales of sea ice anomalies are longer than the time scales of the high-latitude meteorological anomalies.

As an illustration of the effect of the difference in time scales, Fig. 13 shows lagged cross correlations of the monthly Arctic surface temperature and ice extent anomalies. The temperature anomalies are the area-averaged monthly anomalies for the 60–90°N region, while the ice anomalies are those plotted in Fig. 5a. The plotted curves are the cross

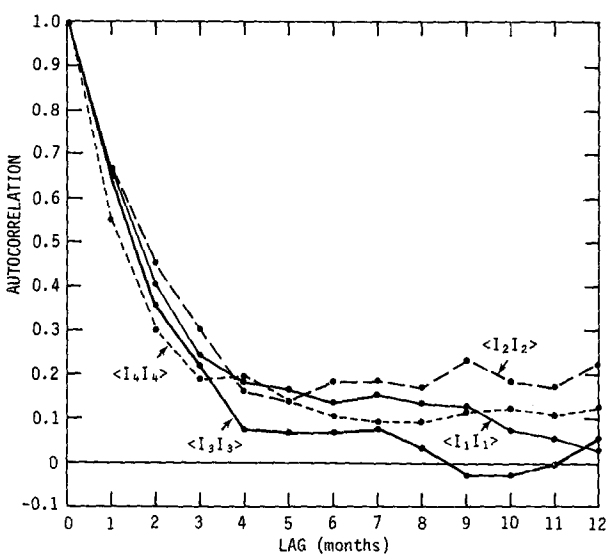

FIG. 11. Autocorrelations at lags 0–12 months of the coefficients of the first four eigenvectors of normalized ice extent.

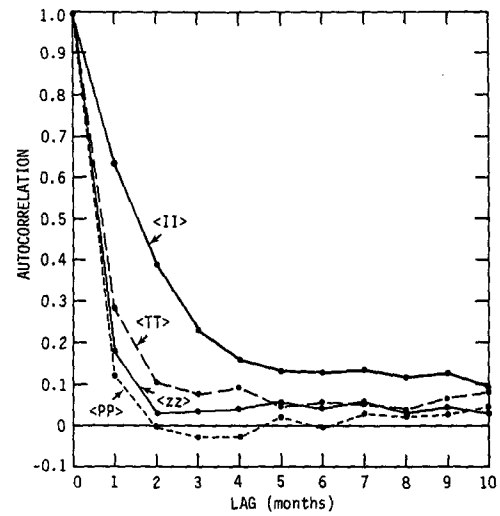

FIG. 12. Autocorrelations at lags 0–10 months of the anomaly fields of sea ice extent (I) and the high-latitude atmospheric fields of sea-level pressure (P), surface temperature (T) and 700 mb height (z). Plotted values are variance-weighted means of the autocorrelations of the first four eigenvector amplitudes of each variable.

correlations computed from 1) the two unsmoothed time series and 2) 24-month running means of the two time series. (The latter curve therefore shows the lagged correlations of the two smoothed series plotted in Figs. 5b and 6.) The relatively low correlations based on the unsmoothed data are not surprising, since the first eigenvector of each variable represents a wavenumber 1 mode in which comparable areas of the Arctic have anomalies that are opposite in sign. In fact, only the third of the temperature eigenvectors (10% of the total temperature variance) describes an anomaly pattern in which the sign of the anomaly is the same over nearly the entire Arctic (Walsh, 1977, Fig. 2). The magnitudes of the cross correlations computed from the smoothed time series are considerably larger at nearly all lags; these correlations remain in the −0.4 to −0.5 range out to larger lags when the lag of the ice is positive.

An analogy can be made between the relative time scales obtained in this study and those obtained by Davis (1976), who used an eigenvector analysis to show that the time scales of North Pacific sea surface temperature anomalies are considerably longer than those of atmospheric sea level pressure anomalies in the same region. Regarding the predictability of sea ice anomalies on the monthly time scale, predictions based on the persistence of ice anomalies will evidently be more successful than predictions based on the persistence of meteorological anomalies. Alternatively, the use of a stochastic climate model may be the most viable approach to establishing the compatibility of the relatively noisy meteorological forcing and the temporally smoother response of the large-scale distribution of sea ice. The latter approach has been used with

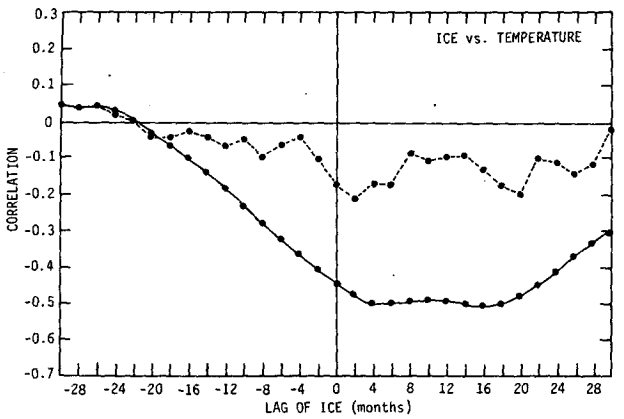

FIG. 13. Lagged cross-correlations of the monthly anomalies of Arctic surface temperature (60–90°N) and ice extent. Data points are evaluated from unsmoothed time series (dashed line) and 24-month running means of both series (solid line). Horizontal axis is number of months by which ice lags temperature.

some success by Frankignoul and Hasselmann (1977) in a study of the effect of high-frequency atmospheric forcing on the lower-frequency response of the thermal structure of the upper ocean.

4. Summary and conclusions

This paper has described the construction and analysis of a data set on Arctic sea ice extent. The major goal of the work was the identification of the dominant spatial and temporal scales of Arctic ice fluctuations over the past 25 years. The findings include the following:

1) Interannual fluctuations in the summer position of the ice margin exceed 5° latitude in most longitudinal sectors. Winter fluctuations are of a comparable magnitude in those longitudes where the ice advance is not blocked by the continental landmasses.

2) The trend in total Arctic ice extent computed from the 300-month sample is positive and statistically significant. The only area in which ice extent has decreased substantially is the Barents Sea.

3) The dominant spatial mode of ice variability is an asymmetric mode in which the North Atlantic anomaly is opposite in sign to the anomaly over the remainder of the polar cap. The second mode corresponds to anomalies of the same sign over nearly the entire hemisphere, while the third mode can be described as a wavenumber 2 departure from normal.

4) The magnitudes of the cross-correlations of the dominant eigenvector amplitudes exceed 0.2 in some portions of the 1–12 month lag range, but no single lagged correlation appears to be of much value for ice forecasting applications.

5) A tendency for anomalies of ice extent to persist for several months is apparent in the lagged autocorrelations of the amplitudes of the dominant ice eigenvectors. The month-to-month persistence of the ice anomalies is considerably greater than the persistence of the high-latitude anomaly fields of sea-level pressure, surface temperature and 700 mb height.

Future work will include a thorough and quantitative evaluation of the relationships between sea ice anomalies and high-latitude meteorological anomalies. Statistical significance of the relations at a positive lag of the ice data will have some implications for the predictability of sea ice extent, while the significance of relations at a positive lag of the atmospheric data would provide observational evidence of a response of the high-latitude atmosphere to a change in ice extent. The general agreement noted in Section 3 between the average surface temperature of the polar cap and total Arctic ice extent is an encouraging sign regarding ice-atmosphere interrelationships. On the other hand, the disparity of the time scales of the atmospheric and sea ice anomalies suggests that the establishment of statistically significant interrelationships will require smoothing or integration of the meteorological data, perhaps in the framework of a stochastic model formulation.

Acknowledgments. This work was sponsored by the National Science Foundation, Division of Polar Programs, through Grants DPP76-15352 and DPP77-17348. Computing facility support was provided by the National Center for Atmospheric Research, which is sponsored by the National Science Foundation. The assistance of J. Lawrence, T. Brown and T. Bennett in the tedious jobs of compiling and digitizing the ice data is appreciated. Thanks are due D. McNeely for typing the manuscript and J. Brother for drafting the figures. We also wish to thank two anonymous reviewers for their very helpful suggestions.

REFERENCES

Ackley, S. R., and T. E. Keliher, 1976: Antarctic sea ice dynamics and its possible climatic effects. *AIDJEX Bull.* **33**, 53–76.

Barnett, D. G., 1979: A practical method of long-range ice forecasting for the north coast of Alaska. *Proc. Symp. Sea Ice Processes and Models*, University of Washington Press (in press).

Björnsson, H., 1969: Sea ice conditions and the atmospheric circulation north of Iceland. *Jökull*, **19**, 11–17.

Budyko, M. I., 1972: The future climate. *Trans. Amer. Geophys. Union*, **53**, 868–874.

Davis, R. E., 1976: Predictability of sea surface temperature and sea level pressure anomalies over the North Pacific Ocean. *J. Phys. Oceanogr.*, **6**, 249–266.

Dehn, W. S., 1972: Alaskan sea ice. *Sea Ice: Proceedings of an International Conference*, Reykjavik, Iceland. T. Karlsson, Ed., National Research Council of Iceland, Reykjavik, 125–129.

Dunbar, M., 1972: Increasing severity of ice conditions in Baffin Bay and Davis Strait and its effect on the extreme limits of ice. *Sea Ice: Proceedings of an International Conference*, Reykjavik, Iceland. T. Karlsson, Ed., National Research Council of Iceland, Reykjavik, 87–93.

Fletcher, J. O., 1968: The influence of Arctic pack ice on climate. *Meteor. Monogr.*, No. 30, Amer. Meteor. Soc., 93–99.

Frankignoul, C., and K. Hasselmann, 1977: Stochastic climate models, Part II: Application to sea-surface temperature anomalies and thermocline variability. *Tellus*, **29**, 289–305.

Haupt, I., and V. Kant, 1976: Satellite ice surveillance studies in the Arctic in relationship to the general circulation. *Proc. Symp. Meteorological Observations from Space, Their Contribution to the First GARP Global Experiment*, COSPAR, ICSU, Paris, 179–187.

Herman, G. F., and W. T. Johnson, 1978: The sensitivity of the general circulation to Arctic sea ice boundaries: A numerical experiment. *Mon. Wea. Rev.*, **106**, 1649–1664.

Kukla, G. J., 1978: Recent changes in snow and ice. *Climatic Change*, J. Gribbin, Ed., Cambridge University Press, 114–129.

Kutzbach, J. E., 1967: Empirical eigenvectors of sea-level pressure, surface temperature and precipitation complexes over North America. *J. Appl. Meteor.*, **6**, 791–802.

Lamb, H. H., 1972: *Climate: Present, Past and Future*, Vol. 1. Methuen and Co., 613 pp.

Mitchell, J. M., B. Dzerdzeevskii, H. Flohn, W. L. Hofmeyr, H. H. Lamb, K. N. Rao and C. C. Wallen, 1966: Climatic change. WMO Tech. Note 79, WMO-No. 195. TP 100, 79 pp.

Sanderson, R. M., 1975: Changes in the area of Arctic sea ice, 1966 to 1974. *Meteor. Mag.*, **104**, 313–323.

Stidd, C. K., 1967: The use of eigenvectors for climatic estimates. *J. Appl. Meteor.*, **6**, 255–264.

Trenberth, K. E., 1975: A quasi-biennial standing wave in the Southern Hemisphere and interrelations with sea surface temperature. *Quart. J. Roy. Meteor. Soc.*, **101**, 55–74.

Untersteiner, N., 1975: Sea ice and ice sheets and their role in climatic variations. The physical basis of climate and climate modelling, GARP Publ. Ser. No. 16, 206–224.

van Loon, H., and J. C. Rogers, 1978: The seasaw in winter temperatures between Greenland and northern Europe. Part I: General description. *Mon. Wea. Rev.*, **106**, 296–310.

——, and J. Williams, 1977: The connection between trends of mean temperature and circulation at the surface: Part IV. Comparison with the upper air and the Antarctic in winter. *Mon. Wea. Rev.*, **105**, 636–647.

Volkov, N. A., and B. A. Sleptsov-Shevlevich, 1971: Cyclic variations of the ice-cover coefficient of the Arctic Seas. Translated in *AIDJEX Bull.*, No. 16, (1972), University of Washington, 1–34.

Walsh, J. E., 1978: Temporal and spatial scales of the Arctic circulation. *Mon. Wea. Rev.*, **106**, 1532–1544.

——, 1977: The incorporation of ice station data into a study of recent Arctic temperature fluctuations. *Mon. Wea. Rev.*, **105**, 1527–1535.

Weare, B. C., A. R. Navato and R. E. Newell, 1976: Empirical orthogonal analysis of Pacific sea surface temperatures. *J. Phys. Oceanogr.*, **6**, 671–678.

Winchester, J. W., and C. C. Bates, 1958: Meteorological conditions and the associated sea ice distribution in the Chukchi Sea during the summer of 1955. *Polar Atmosphere Symposium*, Part I: *Meteorology Section*, R. E. Sutcliffe, Ed., Pergamon Press, 323–334.